HHS Public Access

Author manuscript

Schizophr Res. Author manuscript; available in PMC 2016 June 06.

Published in final edited form as:

Schizophr Res. 2016 April ; 172(1-3): 94–100. doi:10.1016/j.schres.2016.02.031.

Prefrontal neuronal integrity predicts symptoms and cognition in schizophrenia and is sensitive to genetic heterogeneity

Dolores Malaspina[a,*], **Thorsten M. Kranz**[b], **Adriana Heguy**[c], **Sheila Harroch**[d], **Robert Mazgaj**[a], **Karen Rothman**[a], **Adam Berns**[a], **Sumya Hasan**[a], **Daniel Antonius**[e], **Raymond Goetz**[f,h], **Mariana Lazar**[g,i], **Moses V. Chao**[b], and **Oded Gonen**[g,i]

[a]Institute for Social and Psychiatric Initiatives (InSPIRES), Department of Psychiatry, New York University School of Medicine, NY, NY, USA

[b]Skirball Institute of Biomolecular Medicine, Departments of Cell Biology, Physiology & Neuroscience and Psychiatry, New York University, New York, NY 10016, USA

[c]Genome Technology Center, New York University School of Medicine, NY, NY, USA

[d]Department of Psychiatry, New York University School of Medicine, NY, NY, USA

[e]University at Buffalo, Department of Psychiatry, Buffalo, NY, USA

[f]New York State Psychiatric Institute, Division of Clinical Phenomenology, 1051 Riverside Drive, NY, NY, USA

[g]Center for Advanced Imaging Innovation and Research (CAI2R), Department of Radiology, New York University School of Medicine, NY, NY, USA

[h]Columbia University, Department of Psychiatry, NY, NY, USA

[i]Bernard and Irene Schwartz Center for Biomedical Imaging, Department of Radiology, New York University School of Medicine, NY, NY, USA

Abstract

Schizophrenia is a genetically complex syndrome with substantial inter-subject variability in multiple domains. Person-specific measures to resolve its heterogeneity could focus on the variability in prefrontal integrity, which this study indexed as relative rostralization within the anterior cingulate cortex (ACC). Twenty-two schizophrenia cases and 11 controls underwent rigorous diagnostic procedures, symptom assessments (PANSS, Deficit Syndrome Scale) and intelligence testing. All underwent multivoxel MRSI at 3 T to measure concentrations of the neuronal-specific biomarker N-acetylaspartate (NAA) in all of the voxels of the ACC. The

[*]Corresponding author at: Department of Psychiatry, 1 Park Avenue, 8th Floor, Rm 222, New York, NY 10016, USA. ; Email: dolores.malaspina@nyumc.org (D. Malaspina)

Contributors

We certify that authorship for all individuals listed on this manuscript was justified through participation in the following: conception and design (DM, OG, MC), data collection and management (RM, MC, DM, OG, TK), analysis and interpretation of data (TK, RG), drafting of the manuscript (DM, OG, RM), revising the manuscript critically for important intellectual content (all authors), and final approval of the manuscript (all authors).

Conflict of interest

The authors declare no conflict of interest.

concentrations of NAA were separately calculated and then compared across the rostral and caudal subregions to generate a rostralization ratio, which was examined with respect to the study measures and to which cases carried a missense coding polymorphism in *PTPRG*, *SCL39A13*, *TGM5*, *NTRK1* or *ARMS/KIDINS220*. Rostralization significantly differed between cases and controls (χ^2 = 18.40, p < .0001). In cases, it predicted verbal intelligence (r = .469, p = .043) and trait negative symptoms (diminished emotional range (r = −.624, p = .010); curbed interests, r = −.558, p = .025). Rostralization was similar to controls for missense coding variants in *TGM5* and was significantly greater than controls for the *PTPRG* variant carrier. This is the first study examining the utility of MRS metrics in describing pathological features at both group and person-specific levels. Rostralization predicted core illness features and differed based on which signaling genes were disrupted. While future studies in larger populations are needed, ACC rostralization appears to be a promising measure to reduce the heterogeneity of schizophrenia for genetic research and selecting cases for treatment studies.

Keywords

Schizophrenia; Rostralization; Genotype; N-acetylaspartate; Anterior cingulate cortex; Magnetic resonance spectroscopy imaging

1. Introduction

Schizophrenia related psychoses (SRP) are costly and genetically complex brain disorders. Genome wide association studies identify more than a hundred susceptibility loci, but many of these associations are poor and are also associated with bipolar disorder (Frans et al., 2008), autism (Reichenberg et al., 2006) and other conditions (Doherty and Owen, 2014). SRP also shows substantial variability in symptoms, cognition and neuroimaging measures. For person-specific interventions, the field needs simple and effort-independent imaging biomarkers for SRP that are sensitive to established pathophysiological processes. Measures of prefrontal integrity and function have long been sought that would be sensitive to core negative symptoms and cognitive deficits (Egan and Weinberger, 1997). If SRP is a collection of heterogeneous disorders, each strongly influenced by groups of particular susceptibility genes, then a valuable measure would furthermore distinguish gene effects that work through different signaling pathways.

One within-subject and effort independent measure of rostralization is derived as the ratio of N-acetyl-L-aspartate (NAA) in the rostral versus caudal subregion of the anterior cingulate cortex (ACC). NAA is a neuronal-specific metabolite whose concentration can be measured by Magnetic Resonance Spectroscopic Imaging (MRSI) and which indicates neuronal health and integrity. In a previous study (Hardy et al., 2011), we found that the ratio of NAA in the rostral versus caudal subregion of the ACC was significantly lower in cases than controls, consistent with a neuronal deficit in the rostral subregion in schizophrenia. Notably, the cases showed a significantly greater variability in rostralization than the control group, consistent with the etiological heterogeneity of schizophrenia. Some cases had deficient rostralization, driving the significant difference between the cases and controls, but other cases were either similar to controls and or had greater rostralization than controls. Based on

the substantial variability of the biomarker within the cases, the current study re-examined the data with respect to symptoms and cognition and also probed its potential to discriminate among carriers of rare variants in five different major signaling genes. Three were chosen for study in this sample because they harbored de novo missense rare polymorphisms in sporadic schizophrenia cases compared to healthy parents from an Israel sample (*PTPRG*, *SLC39A13*, *TGM5*) (Kranz et al., 2015b) and two selected genes were chosen for their involvement in neurotrophin signaling (*NTRK1*, *ARMS*/*KIDINS220*) (Kranz et al., 2015a).

2. Materials and methods

2.1. Participants

Outpatient cases with a diagnosis of schizophrenia or schizoaffective disorder maintained on steady medication regimens for at least one month were recruited from treatment settings at Bellevue Hospital Center and healthy comparison subjects were recruited from medical center advertisements. All subjects provided written informed consent. Exclusion criteria included presence of internal metal devices, pregnancy, current substance abuse, use of steroidal contraceptives or allergy medications, and history of epilepsy or head injury requiring medical treatment. The study was approved by the Institutional Review Board as a component of an NIMH Challenge Grant to examine genetics and phenotypic variability among schizophrenia cases.

2.2. Assessments

Diagnosis was based on the Diagnostic Interview for Genetic Studies (DIGS) (Nurnberger et al., 1994) and chart reviews. Cross-sectional symptoms were assessed using the 5-factor model of the Positive and Negative Syndrome Scale (PANSS) as Negative, Positive, Dysphoric Mood, Activation (hostility) and Autistic Preoccupation (Kay et al., 1987; White et al., 1997) and enduring (trait) negative symptoms were rated based on the Schedule for the Deficit Syndrome (Kirkpatrick et al., 1989). Wechsler Adult Intelligence Scale (WAIS-III) (Wechsler, 1999) testing yielded Verbal, Performance and full scale Intelligence Quotients (IQs) as well indices for working memory, perceptual organization, processing speed and verbal comprehension. Research assessments were performed by trained raters at the master's level and above who underwent ongoing evaluations, with inter-rater reliability = 0.95 for DSM-IV diagnoses.

2.3. MR data acquisition

For the main imaging outcome, Single photon MRSI scans separately quantified each subject's absolute N-acetyl-L-aspartate (NAA) and other metabolites' concentrations in the entire rostral and caudal ACC subregions, as shown in Fig. 1, and the relative rostral to caudal concentration ratios were calculated. Briefly, experiments were performed with a 3-T whole-body MR imager (Trio; Siemens, Erlangen Germany) and a transmit-receive head-coil (TEM3000; MR Instruments, Minneapolis, Minn) (Hardy et al., 2011). For anatomic reference and guidance of the spectroscopic volume of interest (VOI), a 3D T_1-weighted magnetization-prepared rapid gradient-echo (MP-RAGE) MRI was acquired: repetition time (TR)/echo time (TE)/inversion time, 1360/2.6/800 ms; 256 × 256 × 160 matrix, and 256 ×

256 × 160 mm^3 field of view. The images were reformatted into axial, sagittal and coronal orientations at 1 mm^3 isotropic resolution.

A chemical shift imaging-based procedure subsequently automatically adjusted the first- and second-order magnetic field shims to a whole-head water linewidths of 27 ± 3 Hz in 3–5 min (Tal et al., 2012). An 8 cm anterior–posterior × 5 cm left–right × 3 cm inferior–superior (= 120-cm^3) parallelepiped ^{1}H-MRSI VOI was then image-guided over the ACC, as shown in Fig. 1a, b and excited using point-resolved spectroscopy (PRESS): TR/TE = 1800/35 ms. The VOI was partitioned into 8 × 5 × 6 voxels, a nominal 0.5 cm^3 each, as shown in Fig. 1b. The MR signal was acquired for 256 ms at ± 1 kHz bandwidth. At two averages, the ^{1}H MRSI took 30 min and the entire protocol lasted less than 1 h.

The data was post processed as described by Hardy et al. (2011). The caudal and rostral ACC were outlined and owing to their irregular shape, manually traced on the axial MRI of each subject, as presented in Fig. 1a, b with software then adding the cerebrospinal fluid-partial-volume-corrected (Soher et al., 1998), phased and aligned spectra from all voxels that fell completely or partially within the circumscribed region, as shown in Figs. 1c, d. In addition to NAA, aspartate, glutamate, glutamine, choline, creatine (Cr), myo-inositol, and taurine model functions were used to fit the data. NAA and Cr relative concentrations were determined for the rostral and caudal ACC using the SiTTools-Fitt software package of Soher et al. (1998), as shown in Fig. 1d. While some studies separate NAA from N-acetylaspartylglutamate (NAAG), which modulates glutamate release, we left these signals combined. It was possible to discern NAA from NAAG (5 Hz apart) in the voxels with the best shim, which were in the dorsal ACC, but the two were unresolved in any of the rostral ACC voxels. As it is only about 0.15 of the NAA amplitude, the SNR would be quite low (1–1.5 mM versus 9 mM for the NAA). Since the fidelity of the quantification could be inexact, we treated the NAAG and NAA as a single resonance.

In all subjects the caudal ACC showed better homogeneity than the rostral subregion. This was due to the proximity of the rostral subregion to the air-filled sinuses, which distort the local magnetic field (air-tissue susceptibility broadening). While this effect makes the spectra look “broader” in the rostral ACC and less “sharp” than in in the caudal subregion, the spectral fitting routine adjusted for line-widths and the quality of metabolic quantification is not adversely affected. Of note, the data was not normalized to a common space (e.g. MNI) and subject to automatic analyses because SPM was only used to segment white matter, gray matter, and cerebrospinal fluid to correct for the partial volume of CSF in each voxel, which is metabolite free. As MRS is of much lower resolution, the matrix size and the alignment process would have distorted the metabolic information. Instead the spectroscopy and anatomical data were aligned in each subject's space and spectra and the associated metrics (i.e., metabolites' concentrations) were obtained in this space.

2.4. Targeted exome capture

This study examined the rostralization ratios of cases with missense coding rare variants (MAF < .01) in any of five genes compared to a group of cases with common sequences in all of these genes. One case each harbored rare variants and novel missense variants in transglutaminase 5 (*TGM5*), zinc transporter ZIP13 (*SLC39A13*), receptor-type tyrosine-

protein phosphatase gamma (*PTPRG*), ankyrin rich membrane spanning protein (*ARMS*/*KIDINS220*) and tyrosine receptor kinase A (*NTRK1*) (Kranz et al., 2015a; Kranz et al., 2015b).

2.5. Data analysis

Data were entered and verified using the SIR Database Management Software (SIR 2002, SIR Pty Ltd) and analyzed with IBM SPSS (Statistics 22). Descriptive statistics and distributions of all continuous and categorical measures were examined to identify features impacting inferential methods. Demographics were compared using t-test and chi-square statistics. One case each with rare missense coding variants in *TGM5*, *SLC39A13*, *PTPRG*, *ARMS*/*KIDINS220* and *NTRK1* were compared to the group of cases that did not harbor such variants in any of these genes and to the group of controls. Rostral to caudal ACC metabolites were calculated as ratios (r/d) between the concentrations in the ACC subregions and compared using a multivariate ANCOVA. WAIS-III scores were examined using two MANCOVAs, one for Verbal and Performance IQs, and another for the four indices. Sex and age were included as covariates in all ANOVAS. PANSS factors and items from the Schedule for the Deficit Syndrome were similarly examined.

3. Results

3.1. Group measures

Case and control groups were similar in sex ratio (13/22: 7/11 males) and mean age (39.3 ± 10.5 vs. 35.3 ± 10.4 years, t = 1.04, df = 31, p = .308). An overall MANCOVA analysis did not reveal group differences on global WAIS-III scores (Wilks' Lambda p = .121). However, significant between-subjects effects were demonstrated for Verbal IQ (p = .046) and marginal differences were shown for Performance IQ (p = .079). MANCOVA analyses showed significant group differences for the four WAIS Indices (Wilks' Lambda p = .017), with particularly robust between-subjects effects for the Working Memory (p = .008) and Processing Speed (p = .008) Indices, with only marginal effects for the Verbal Comprehension Index (p = .075). Controls outperformed cases in all cognitive measures.

The groups also did not significantly differ in their mean rostral or caudal ACC volume or in the mean rostral or caudal subregion NAA concentration (Table 1), but the rostral to caudal subregion comparisons ratios of NAA showed deficient rostral concentrations in the cases compared to controls (0.90 ± 0.17 vs. 1.03 ± .09, F[1/29] = 5.77, p = .023). Among the cases, Verbal IQ correlated with rostralization (r = .469, p = .043), such that relative rostral deficits were related to lesser verbal intelligence in the cases, these being unassociated in controls (r = −.314, p = .347). Verbal comprehension was similarly correlated with rostralization in cases (r = .481, p = .037), but not in the controls; the control group conversely showed that relatively lower rostral NAA (hence greater caudal NAA) predicted the Verbal index (r = −.870, p < .001). A Fisher's exact test revealed a significantly different relationship for the case and control groups (Fisher's R to Z: $\chi^2 = 18.40$, p < .0001). As to symptoms, decreased rostralization predicted the magnitude of pathology in the trait-related deficit syndrome items of diminished emotional range (r = −.624, p = .010) and curbing of

interests (r = −.558, p = .025). No trait (PANSS) symptoms were associated with rostral deficit.

3.2. Genotypes

The mean rostralization ratios for healthy controls, cases with respective rare variant carriers in *TGM5*, *SLC39A13*, *PTPRG*, *ARMS*/*KIDINS220*, *NTRK1* and the 9 cases with no rare missense coding variants in these genes are shown in Fig. 2. A significant group effect was demonstrated for ACC rostralization across the controls, cases with rare variants and other cases (F = 3.66, p = .02). The rostralization ratio for *PTPRG* was greater than controls and for *TGM5* it was similar to controls. *SLC39A13*, *ARMS*/*KIDINS220* and *NTRK1* carriers had reduced rostralization compared to controls. Examining the Cr ratio across the rostral and caudal ACC also showed significant group effects with the same relative pattern as for NAA. There was only a trend effect for choline across the groups and none for myo-inositol, although it was consistent with a greater rostral concentration for *PTPRG* and *TGM5* carriers as well. All of the rare missense coding polymorphisms in these genes were located in functional protein or protein interaction domains aside from those in *TGM5* (Table 2). The *TGM5* carrier had two rare missense coding polymorphisms.

4. Discussion

This study demonstrated that deficient rostralization is significantly correlated with verbal decrements and with trait-negative symptoms in schizophrenia, which are the core illness features. Moreover, rostralization was sensitive to certain genotypes. While carriers of zinc transporter (*SLC39A13*) and neurotrophin signaling gene variants (*NTRK1* and *ARMS*/*KIDINS220*) had similar rostralization deficits in comparison to the non-carrier cases in this sample, the *TGM5* variant carrier had the same profile as healthy controls and the *PTPRG* missense polymorphism carrier conversely demonstrated greater rostralization than any other case or control. Interestingly, the rare missense coding polymorphisms in *ARMS*/*KIDINS220* and *NTRK1* are located in functional protein domains, namely the sterile alpha motif and the transmembrane domain. NTRK1 and ARMS/KIDINS220 are two proteins that are located in the same signaling cascade. Both proteins are co-expressed in cholinergic projections (Duffy et al., 2011). Interestingly, in a study investigating protein levels of NTRK1 in cortical regions in cases diagnosed with mild Alzheimer's disease it was shown that NTRK1 levels are reduced about 50% in comparison to controls (Counts et al., 2004). Since it was shown that the ACC expressed cholinergic m2 receptors and its activity gets modulated by acetylcholine (Medalla and Barbas, 2012), rare missense coding polymorphisms in two proteins of the same signaling pathway on the top of the hierarchy might alter their activity and thus partially explain the reduced rostralization in these cases.

Another interesting observation was the absence of novel missense coding mutations in the other neurotrophin receptors *NTRK2* (*TrkB*) and *NTRK3* (*TrkC*).

Rostralization, based on these person-specific measurements of the NAA concentrations in the rostral compared to the caudal ACC subregions, also revealed a central relationship to the pathogenic processes producing illness features of schizophrenia, demonstrated by its significant correlations to verbal capacity, including comprehension and intelligence, and to

trait-negative symptoms of the deficit syndrome. As rostralization ratios differed based on which high impact gene was harbored, the measure may be useful for apportioning the effect of genotypic variability on prefrontal integrity, as well as for grouping cases for treatment studies.

Specific influential genes are expected to account for variability across many illness features, including symptom severity and cognition. In the cases without the rostralization deficit (*PTPRG* and *TGM5*), different processes than prefrontal deficits may underlie their psychotic conditions. Carriers of missense coding variants in these genes respectively showed deficits in working memory and processing speed, respectively (data not shown), which may be specific psychosis related pathways that do not entail rostralization deficits as defined through this imaging measure. The rostralization profile in the cases carrying missense-coding variants in the zinc transporter and neurotrophin genes were similar to the other non-carrier cases in this sample. Further in vitro studies will be needed to confirm pathophysiology of these genes in the disease. For zinc transporter related pathophysiologies, specific treatments could relate to supplementation of zinc.

These findings support a high value to this imaging biomarker in shedding light on whether different missense coding variants act in common or disparate pathways to increase the risk for the disease. Interestingly, all of the genes investigated in this study reveal a high expression pattern in the central nervous system and especially in the limbic system, including the addiction and reward-related brain regions like the ventral tegmentum area (VTA) (Greene, 2006; Sulzer, 2011), the amygdala, an anxiety-correlated brain region (Dunsmoor and Paz, 2015), and the hippocampus (Molendijk et al., 2012). Especially the neurotrophin receptors, including the scaffold protein ARMS/KIDINS220 and NTRK1, are known for their important functions in neuronal network integrity and synaptic plasticity. ARMS/KIDINS220 is an immediate downstream scaffold protein interacting with the Trk receptors and gets phosphorylated upon nerve growth factor (NGF) and brain derived neurotrophic factor (BDNF) stimulation, and is important for sustained MAPK signaling, which supports neuronal viability (Arevalo et al., 2004). PTPRG is a tyrosine receptor phosphatase and interacts with a number of cell adhesion molecules and facilitates synaptic stability (Bouyain and Watkins, 2010) and has been previously considered to be a susceptibility locus for schizophrenia (Schizophrenia Psychiatric Genome-Wide Association Study, 2011). Mutations in the zinc transporter SLC39A13 cause an extracellular matrix-affecting disease (Fukada et al., 2008). TGM5 is a transglutaminase expressed in the mitochondria that has been associated with acral peeling skin syndrome (Pigors et al., 2012). While TGM5 has not been associated with schizophrenia, it is of interest that the chemical profile of rostralization was similar for the affected case and the group of controls suggesting some different mechanism.

ACC rostralization ratios may be useful for apportioning genotypic variability, defining pathophysiologies and in grouping cases for treatment studies.

Another strength of using NAA is that it yields a quantitative imaging biomarker of neuronal integrity (Baslow, 2003; Kraepelin, 1919) and the current measure generates a quantitative ratio. Rostralization is sensitive to the severity of trait-negative symptoms and may index the

neuronal underpinnings of the illness features at the core of schizophrenia. Kraepelin (1919) described avolition as “weakened volitional impulse” and considered it to be the central defect in schizophrenia. It predicts a poor outcome in psychosis, including asociality, decreased interests, desires, goals and self-initiated, purposeful behavior (Jogems-Kosterman et al., 2001; Morrens et al., 2007) such as: motor retardation/physical anergia (Brewer et al., 1996), decreased grooming and hygiene (Vuksic-Mihaljevic et al., 1998), and observable decreases in work, school, vocation, leisure, and social activities (Malaspina et al., 2014). The significant association of decreased rostralization with diminished emotional range, curbing of interests, and restricted affect in this group of cases suggests it may have utility for research aimed at describing particular domains of pathology rather than diseases per se. Research Domain Criteria (RDoC) studies of enduring negative symptoms could benefit from this imaging approach. Further analyzing these phenotypic differences phenotype may allow for advanced understanding of heterogeneity of schizophrenia subtypes, and can ultimately lead to more effective and individualized treatments.

This person-specific, effort-independent measure, requiring only a single MRI scan, is sensitive for the diagnosis of schizophrenia and subgroups that may differ in their etiopathophysiology for schizophrenia and may thus also be useful for evaluating responses to treatment. The finding of reduced rostralization in association with rare variants in putative psychosis genes as well as with cognitive deficits and negative symptoms suggests that this biomarker may be particularly promising as an outcome measure in treatment studies. If so, longitudinal studies will show normalization of the rostral cingulate neuronal density in association with clinical improvement. On the other hand, the biomarker may reflect an unchanging trait, perhaps reflecting an early neurodevelopmental compromise. If so, it might still have value in specifying subgroups of psychotic cases with a shared etiopathology for precision-based treatment studies. With such measures, psychosis can no longer be defined as a functional condition due to the absence of organic lesions.

Such measures are urgently needed in the field. As the relevant illness features associated with rostralization are core features of schizophrenia, the measure may have some utility for future diagnostic approaches and the elucidation of genetic pathways in addition to treatment studies.

Acknowledgments

N/A.

Role of funding source

This work was supported by the National Institutes of Health Grants R01-MH59114 (DM), RC1-MH088843 (DM), 5K24MH001699 (DM), NYU CTSI UL1TR000038 (DM), MH086651 (MVC), and EB01015 and performed in part under the rubric of the Center for Advanced Imaging Innovation and Research (CAI^{2}R, www.cai2r.net), a NIBIB Biomedical Technology Resource Center (NIH P41 EB017183).

References

Arevalo JC, Yano H, Teng KK, Chao MV. A unique pathway for sustained neurotrophin signaling through an ankyrin-rich membrane-spanning protein. EMBO J. 2004; 23(12):2358–2368. [PubMed: 15167895]

Baslow MH. N-acetylaspartate in the vertebrate brain: metabolism and function. Neurochem. Res. 2003; 28(6):941–953. [PubMed: 12718449]

Bouyain S, Watkins DJ. The protein tyrosine phosphatases PTPRZ and PTPRG bind to distinct members of the contactin family of neural recognition molecules. Proc. Natl. Acad. Sci. U. S. A. 2010; 107(6):2443–2448. [PubMed: 20133774]

Brewer WJ, Edwards J, Anderson V, Robinson T, Pantelis C. Neuropsychological, olfactory, and hygiene deficits in men with negative symptom schizophrenia. Biol. Psychiatry. 1996; 40(10):1021–1031. [PubMed: 8915562]

Doherty JL, Owen MJ. Genomic insights into the overlap between psychiatric disorders: implications for research and clinical practice. Genome Med. 2014:6. [PubMed: 24479626]

Duffy AM, Schaner MJ, Wu SH, Staniszewski A, Kumar A, Arevalo JC, Arancio O, Chao MV, Scharfman HE. A selective role for ARMS/Kidins220 scaffold protein in spatial memory and trophic support of entorhinal and frontal cortical neurons. Exp. Neurol. 2011; 229(2):409–420. [PubMed: 21419124]

Dunsmoor JE, Paz R. Fear generalization and anxiety: behavioral and neural mechanisms. Biol. Psychiatry. 2015 Sep 1; 78(5):336–343. http://dx.doi.org/10.1016/j.biopsych.2015.04.010 PubMed PMID: 25981173. [PubMed: 25981173]

Egan MF, Weinberger DR. Neurobiology of schizophrenia. Curr. Opin. Neurobiol. 1997; 7(5):701–707. [PubMed: 9384552]

Frans EM, Sandin S, Reichenberg A, Lichtenstein P, Langstrom N, Hultman CM. Advancing paternal age and bipolar disorder. Arch. Gen. Psychiatry. 2008; 65(9):1034–1040. [PubMed: 18762589]

Fukada T, Civic N, Furuichi T, Shimoda S, Mishima K, Higashiyama H, Idaira Y, Asada Y, Kitamura H, Yamasaki S, Hojyo S, Nakayama M, Ohara O, Koseki H, dos Santos HG, Bonafe L, Ha-Vinh R, Zankl A, Unger S, Kraenzlin ME, Beckmann JS, Saito I, Rivolta C, Ikegawa S, Superti-Furga A, Hirano T. The zinc transporter SLC39A13/ZIP13 is required for connective tissue development; its involvement in BMP/TGF-β signaling pathways. PLoS One. 2008; 3(11):e3642. [PubMed: 18985159]

Greene JG. Gene expression profiles of brain dopamine neurons and relevance to neuropsychiatric disease. J. Physiol. 2006; 575(Pt 2):411–416. [PubMed: 16740610]

Hardy CJ, Tal A, Babb JS, Perry NN, Messinger JW, Antonius D, Malaspina D, Gonen O. Multivoxel proton MR spectroscopy used to distinguish anterior cingulate metabolic abnormalities in patients with schizophrenia. Radiology. 2011; 261(2):542–550. [PubMed: 21900615]

Jogems-Kosterman BJM, Zitman FG, Van Hoof JJM, Hulstijn W. Psychomotor slowing and planning deficits in schizophrenia. Schizophr. Res. 2001; 48(2–3):317–333. [PubMed: 11295384]

Kay SR, Fiszbein A, Opler LA. The Positive and Negative Syndrome Scale (PANSS) for schizophrenia. Schizophr. Bull. 1987; 13(2):261–276. [PubMed: 3616518]

Kirkpatrick B, Buchanan RW, Mckenney PD, Alphs LD, Carpenter WT. The Schedule for the Deficit Syndrome — an instrument for research in schizophrenia. Psychiatry Res. 1989; 30(2):119–123. [PubMed: 2616682]

Kraepelin, E. Dementia Praecox and Paraphrenia. Livingstone, Munich, Germany: 1919.

Kranz TM, Goetz RR, Walsh-Messinger J, Goetz D, Antonius D, Dolgalev I, Heguy A, Seandel M, Malaspina D, Chao MV. Rare variants in the neurotrophin signaling pathway implicated in schizophrenia risk. Schizophr. Res. 2015a; 168(1–2):421–428. [PubMed: 26215504]

Kranz TM, Harroch S, Manor O, Lichtenberg P, Friedlander Y, Seandel M, Harkavy-Friedman J, Walsh-Messinger J, Dolgalev I, Heguy A, Chao MV, Malaspina D. De novo mutations from sporadic schizophrenia cases highlight important signaling genes in an independent sample. Schizophr. Res. 2015b; 166(1–3):119–124. [PubMed: 26091878]

Malaspina D, Walsh-Messinger J, Gaebel W, Smith LM, Gorun A, Prudent V, Antonius D, Trémeau F. Negative symptoms, past and present: a historical perspective and moving to DSM-5. Eur. Neuropsychopharmacol. 2014; 24(5):710–724. [PubMed: 24314851]

Medalla M, Barbas H. The anterior cingulate cortex may enhance inhibition of lateral prefrontal cortex via M2 cholinergic receptors at dual synaptic sites. J. Neurosci. 2012; 32(44):15611–15625. [PubMed: 23115196]

Molendijk ML, van Tol MJ, Penninx BW, van der Wee NJ, Aleman A, Veltman DJ, Spinhoven P, Elzinga BM. BDNF val66met affects hippocampal volume and emotion-related hippocampal memory activity. Transl. Psychiatry. 2012; 2:e74. [PubMed: 22832736]

Morrens M, Hulstijn W, Sabbe B. Psychomotor slowing in schizophrenia. Schizophr. Bull. 2007; 33(4):1038–1053. [PubMed: 17093141]

Nurnberger JI Jr, Blehar MC, Kaufmann CA, York-Cooler C, Simpson SG, Harkavy-Friedman J, Severe JB, Malaspina D, Reich T. Diagnostic interview for genetic studies. Rationale, unique features, and training. NIMH Genetics Initiative. Archives of General Psychiatry. 1994; 51(11): 849–859. (discussion 863–844). [PubMed: 7944874]

Pigors M, Kiritsi D, Cobzaru C, Schwieger-Briel A, Suarez J, Faletra F, Aho H, Makela L, Kern JS, Bruckner-Tuderman L, Has C. TGM5 mutations impact epidermal differentiation in acral peeling skin syndrome. J. Investig. Dermatol. 2012; 132(10):2422–2429. [PubMed: 22622422]

Reichenberg A, Gross R, Weiser M, Bresnahan M, Silverman J, Harlap S, Rabinowitz J, Shulman C, Malaspina D, Lubin G, Knobler HY, Davidson M, Susser E. Advancing paternal age and autism. Arch. Gen. Psychiatry. 2006; 63(9):1026–1032. [PubMed: 16953005]

Schizophrenia Psychiatric Genome-Wide Association Study, C. Genome-wide association study identifies five new schizophrenia loci. Nat. Genet. 2011; 43(10):969–976. [PubMed: 21926974]

Soher BJ, Young K, Govindaraju V, Maudsley AA. Automated spectral analysis—III: application to in vivo proton MR spectroscopy and spectroscopic imaging. Magn. Reson. Med. 1998; 40(6):822–831. [PubMed: 9840826]

Sulzer D. How addictive drugs disrupt presynaptic dopamine neurotransmission. Neuron. 2011; 69(4): 628–649. [PubMed: 21338876]

Tal A, Kirov II, Grossman RI, Gonen O. The role of gray and white matter segmentation in quantitative proton MR spectroscopic imaging. NMR Biomed. 2012; 25(12):1392–1400. [PubMed: 22714729]

Vuksic-Mihaljevic Z, Mandic N, Barkic J, Laufer D. Schizophrenic disorder and social functioning. Psychiatry Clin. Neurosci. 1998; 52(1):21–27. [PubMed: 9682929]

Wechsler DS. Wechsler Abbreviated Scale of Intelligence. 1999

White L, Harvey PD, Opler L, Lindenmayer JP. Empirical assessment of the factorial structure of clinical symptoms in schizophrenia. A multisite, multimodel evaluation of the factorial structure of the Positive and Negative Syndrome Scale. The PANSS Study Group. Psychopathology. 1997; 30(5):263–274. [PubMed: 9353855]

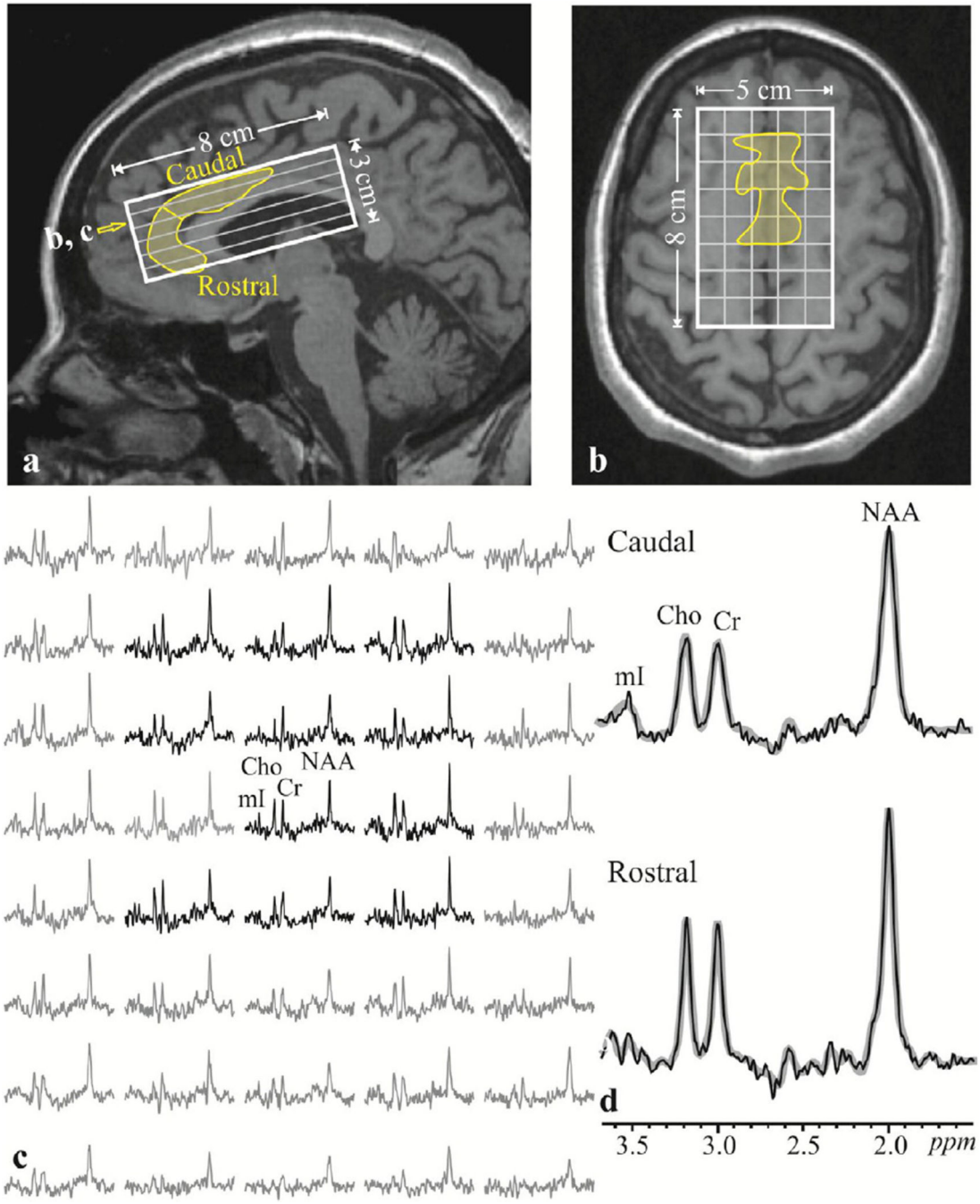

Fig. 1.

Top: Sagittal (a) and axial (b) T1-weighted MP-RAGE MRI from a 30 year old female schizophrenia patient superimposed with the 5 × 8 × 3 cm^3 VOI and 5 × 8 × 6 voxel grid (solid white and gray lines) and the ACC (yellow outline). Open yellow arrow on a denotes the level of b and c. Bottom, left c: Real part of the 5 × 8 axial ^1H spectra matrix from the VOI on b. Spectra represent 0.5 cm^3 voxels and all are on common frequency and intensity scales. Spectra within the ACC (yellow outline in b) are black, outside (not included in the analysis) gray. Note the good SNR and excellent spectral resolution (5.3 ± 1.2 Hz linewidth)

from these high spatial resolution voxels. Bottom Right, d: Real part of the ^{1}H spectra sums from all the voxels within the caudal (top) and rostral (bottom) regions of the ACC (thin black line), superimposed with the spectral fit function (thick gray line) used for quantification. Note the excellent SNR of the spectra and the (consequent) quality of the fit.

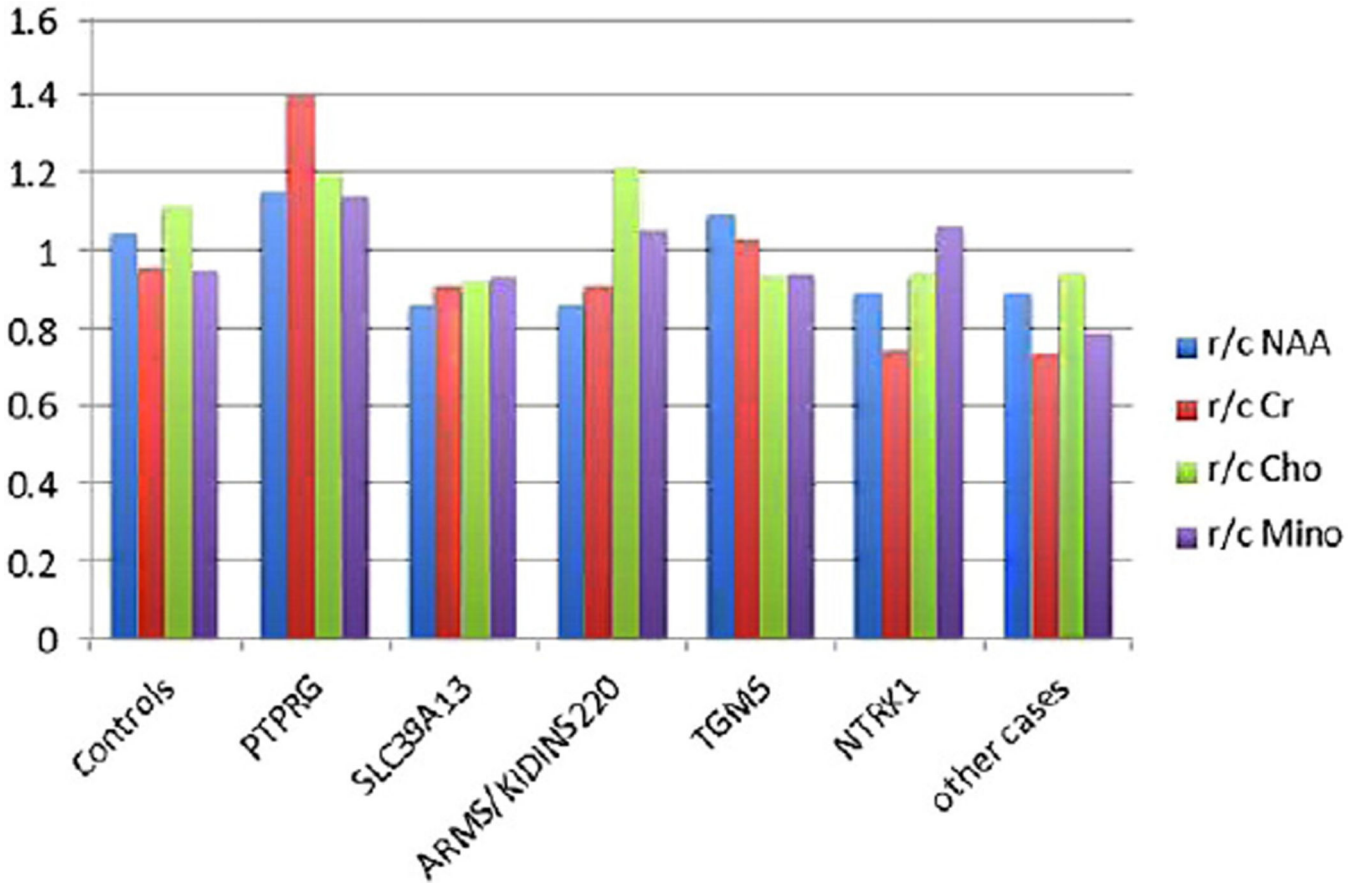

Fig. 2.

Neurochemical concentrations in the rostral versus caudal subregions of the ACC separately for healthy controls; cases who harbor mutations/rare variants in signaling genes: PTPRG, SLC39A13, ARMS/KIDINSS220, TGM5 and NTRK1; and other cases having common variants in all of these particular genes. ANOVAs comparing groups: for NAA: F = 3.66, p = .02; Cr = 2.83, p = .04; Cho = 2.53, p = .06; myoinositol = 1.87, p = .15.

Table 1

Demographic characteristics, MRS 3 T ACC NAA metabolic concentrations and WAIS IQ and Indices in healthy controls and schizophrenia cases.

	Healthy controls	**Schizophrenia cases**	**Diagnosis effect**
	N = 11	**N = 22**	
Sex ratio (M:F)	7:4	13:9	$\chi^2 = 0.06$, df = 1, p = .801
	Healthy controls	Schizophrenia cases	Diagnosis effect
	MN ± sd	MN ± sd	
Age	35.3 ± 10.4	39.3 ± 10.5	t = 1.04, df = 31, p = .308
ACC metabolites	Healthy controls	Schizophrenia cases	F, df, p
	MN ± sd	MN ± sd	
		Wilks' Lambda=	2.72, 2/28, .084
Rostral NAA	6.60 ± 0.83	6.23 ± 1.28	0.79, 1/29, .383
Caudal NAA	6.47 ± 1.10	7.10 ± 1.62	1.11, 1/29, .301
		Wilks' Lambda=	0.59, 2/28, .564
Rostral creatinine	5.50 ± 0.79	5.66 ± 1.35	0.09, 1/29, .764
Caudal creatinine	5.80 ± 1.13	6.33 ± 1.55	1.00, 1/29, .325
R/C NAA ratio	1.03 ± .08	0.90 ± .17	5.77, 1/29, .023
R/C CR ratio	.97 ± .16	.91 ± .18	1.02, 1/29, .321
WAIS IQ & Indices	Healthy controls	Schizophrenia cases	F, df, p
	MN ± sd	MN ± sd	
IQ		Wilks' Lambda F[1/26] = 2.30, p = .121	
Verbal IQ	106.5 ± 8.8	93.7 ± 15.4	4.38, 1/26, .046
Performance IQ	99.2 ± 12.4	88.3 ± 14.9	3.34, 1/26, .079
Indices		Wilks' Lambda=	3.75, 4/23, .017
Working Memory Index	106.9 ± 14.8	89.0 ± 15.32	8.15, 1/26, .008
Verbal Comprehension	108.0 ± 6.8	96.7 ± 15.3	3.43, 1/26, .075
Perceptual Organization	98.6 ± 12.9	89.6 ± 16.5	1.43, 1/26, .008
Processing Speed	101.4 ± 15.2	86.6 ± 14.4	8.30, 1/26, .008

Table 2

Description of rare missense coding polymorphisms in each case.

Case	Chr	Genomic pos. (hg19)	Transcripts/AA exchange	Variant ID	1000g2012apr_all (%)	1000G_Case_Ethnicity (%)	Polyphen-2 score	Prediction	Functional domain
***PTPRG* (736 kb)**									
1010	3	62153771	PTPRG:NM_002841:exon8:c.C967T:p.R323C	rs142366357	0.05	1 (AFR)	0.876	Possibly damaging	Immediately adjacent to alpha carbonic anhydrase
***SLC39A13* (9 kb)**									
1034	1	47431764	SLC39A13:NM_001128225:exon2:c.G119A:p.R40Q,SLC39A13:NM_152264:exon2:c.G119A:p.R40Q	rs35741412	1	0.2 (AFR)	0.02	Benign	None, located in cytoplasm
***TGM5* (34 kb)**									
1033	15	43525791	TGM5:NM_004245:exon11:c.T1724C:p.V575A,TGM5:NM_201631:exon12:c.T1970C:p.V657A	rs80058195	1	− (AJ)	0.137	Benign	Ig like domain
1033		43527022	TGM5:NM_004245:exon10:c.A1574C:p.E525A,TGM5:NM_201631:exon11:c.A1820C:p.E607A	rs80192997		− (AJ)	0.984	Probably damaging	
***ARMS/KIDINS220* (112 kb)**									
1022	2	8873731	KIDINS220:NM_020738:exon29:c.C3896G:p.A1299G	rs76164009	0.27	1.7 (AFR)	0	Benign	Sterile alpha motif
***NTRK1* (66 kb)**									
1006	1	156844777	NTRK1:NM_001012331:exon10:c.G1313A:p.R438Q,NTRK1:NM_001007792:exon11:c.G1223A:p.R408Q,NTRK1:NM_002529:exon11:c.G1331A:p.R444Q	rs56320207	1	3 (AFR)	0.03	Benign	Transmembrane domain